

Combined obliquity and precession pacing of late Pleistocene deglaciations

Peter Huybers¹

Milankovitch¹ proposed that Earth resides in an interglacial state when its spin axis both tilts to a high obliquity and precesses to align the Northern Hemisphere summer with Earth's nearest approach to the Sun. This general concept has been elaborated into hypotheses that precession², obliquity^{3,4} or combinations of both^{5–8} could pace deglaciations during the late Pleistocene^{9,10}. Earlier tests have shown that obliquity paces the late Pleistocene glacial cycles^{4,11} but have been inconclusive with regard to precession, whose shorter period of about 20,000 years makes phasing more sensitive to timing errors^{4,11,12}. No quantitative test has provided firm evidence for a dual effect. Here I show that both obliquity and precession pace late Pleistocene glacial cycles. Deficiencies in time control that have long stymied efforts to establish orbital effects on deglaciation are overcome using a new statistical test that focuses on maxima in orbital forcing. The results are fully consistent with Milankovitch's proposal but also admit the possibility that long Southern Hemisphere summers contribute to deglaciation.

During the late Pleistocene—roughly over the past million years—Northern Hemisphere continental ice has alternately covered much of northern North America and Fennoscandia and then retreated to today's relatively ice-free conditions at intervals of approximately 100,000 years (100 kyr). The cause of these massive shifts in climate remains unclear not for lack of models, of which there are now over thirty^{2–10,13,14}, but for want of means to choose among them. Previous statistical tests have demonstrated that obliquity paces the ~100-kyr glacial cycles^{4,11}, helping narrow the list of viable mechanisms, but have been inconclusive with respect to precession (that is, $P > 0.05$) because of small sample sizes and uncertain timing^{4,11,12}.

Whether precession influences the ~100-kyr glacial–interglacial cycles is not obvious. Precession alters diurnal average insolation intensity by as much as 30 W m^{-2} on a given day of the year, suggesting a powerful forcing, and its signature clearly appears in proxy records of temperature and ice volume at ~20-kyr periods². However, its insolation anomalies are exactly counterbalanced across the seasons so that annual insolation at any latitude is independent of precession¹⁵. Furthermore, proxies of early-Pleistocene glaciation show strong obliquity and little precession variability, indicating that precession had negligible influence during this next-most-recent epoch of glaciation¹⁶, though see ref. 17 for another view.

Here, I test whether anomalously large combinations of precession and obliquity forcing combine to determine when deglaciations occurred during the late Pleistocene. The test involves three steps. The first is to estimate the timing of terminations, for which I use a composite $\delta^{18}\text{O}$ record whose chronology is derived by linearly interpolating age with depth between the last deglaciation and radiometrically dated geomagnetic reversals¹¹. Timescale uncertainty over the past million years is estimated by running a stochastic sediment accumulation rate model¹¹ that also accounts for uncertainties in the alignment of features between $\delta^{18}\text{O}$ stratigraphies, decompaction of sediment, transport times of $\delta^{18}\text{O}$ within the ocean, and geomagnetic reversal ages. The age of the Matuyama–Brunhes geomagnetic reversal was earlier assumed to be known to within ± 2 kyr (one standard deviation, 1 s.d.)¹¹, but to

account for uncertainty in the ^{40}K decay constant^{18,19}, it is now represented as occurring at 780 ± 8 kyr (1 s.d.). Terminations are identified by local maxima in the time rate-of-change of the $\delta^{18}\text{O}$ record that exceed a value of 0.095‰ per kyr, giving the usual termination features²⁰ except that termination 3 contains two parts that are labelled 3a and 3b (Fig. 1a). (Thresholds ranging between 0.07‰ and 0.17‰ per kyr would give different numbers of terminations but give similarly significant results.) The average uncertainty in the age of the 12 identified termination features is 8 kyr (1 s.d.), with older ages generally being more uncertain.

The second step is to define an insolation forcing function, of which there are many varieties^{1,2,16}. For present purposes only the relative shape of the forcing function is needed, and a generic and broadly representative formulation⁵ can be adopted:

$$\mathcal{F}_t = \alpha^{1/2} e_t \sin(\omega_t - \phi) + (1 - \alpha)^{1/2} \varepsilon_t \quad (1)$$

Here e represents eccentricity, ω is the angle from vernal equinox to perihelion, ε is obliquity, subscript 't' indicates time, and ϕ and α are adjustable parameters that respectively control the phase of precession and the relative contributions from precession and obliquity. Both $e_t \sin(\omega_t - \phi)$ and ε_t are normalized to zero-mean and unit variance such that \mathcal{F}_t also has unit variance. Milankovitch¹, along with many subsequent authors^{5–7,9,10,16}, called upon anomalies in incoming solar radiation during the Northern Hemisphere summer to determine whether the Northern Hemisphere is glaciated. Increased insolation intensity during Northern Hemisphere summer results from greater obliquity and a phase of precession that brings Earth closer to the Sun during that season, and can be represented by setting $\phi = 0^\circ$ and $\alpha = 0.5$. The resulting structure of \mathcal{F}_t (Fig. 1b) shares more than 99% of its variance in common with both Milankovitch's caloric summer half-year insolation¹ at 65° N and summer energy¹⁶ at 65° N when using a threshold of 350 W m^{-2} , providing a suitable representation of the hypothesis that Northern Hemisphere summer insolation controls glaciation.

In the third and final step, forcing maxima in \mathcal{F}_t that correspond most closely in time with each termination are compared against forcing maxima not associated with terminations (Fig. 1b). In particular, the median value of the non-termination maxima is subtracted from the median value of the termination maxima, yielding $\delta m = 0.89$. Unlike the Rayleigh's R statistic (relied upon for previous tests of orbital influence upon deglaciation^{4,11,12,21}), timing errors do not affect δm unless they cause the wrong forcing cycles to be identified. Median values are also less sensitive to timing errors because outliers generally have no effect.

The significance of δm is assessed within the context of a null hypothesis H_0 , that termination timing is independent of \mathcal{F}_t , and an alternative hypothesis H_1 , that terminations tend to occur when the maxima in \mathcal{F}_t are anomalously large. For purposes of comparison with earlier work⁴, a modified random walk representing ice-volume variability is adopted for the null hypothesis:

$$v_t = v_{t-1} + \eta_t \quad \text{and if } v_t \geq h_t \text{ then terminate} \quad (2)$$

Ice volume v_t accumulates by a random increment η_t during each 1-kyr time step, until a threshold h_t is passed, and the termination of all ice is

¹Harvard University, Department of Earth and Planetary Sciences, 20 Oxford Street, Cambridge, Massachusetts 02138, USA.

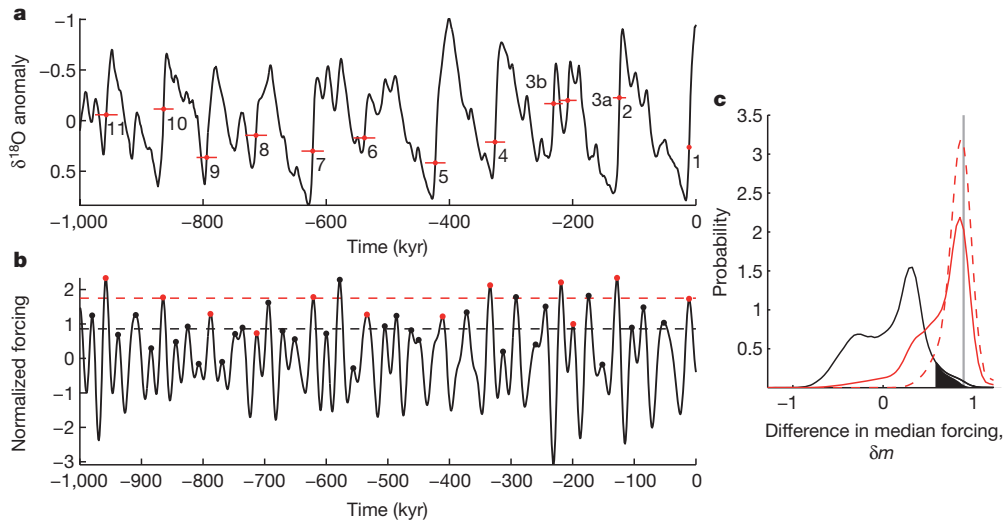


Figure 1 | Test of the Milankovitch hypothesis. **a**, Anomalies in $\delta^{18}\text{O}$ on a depth-derived timescale¹¹. Terminations are identified when rates of change exceed 0.95‰ per kyr and are pinpointed at their maximum rate of change (red dots, with 2 s.d. time-uncertainty indicated by the horizontal bars). **b**, Orbital forcing containing equal amounts of obliquity and climatic precession variability and the contribution of climatic precession peaking during the Northern Hemisphere summer solstice. The forcing maximum nearest each

prescribed to occur over the ensuing 10 kyr. Defining $h_t = 90$ units, randomly initializing ice volume between 0 and 90 units, and drawing η_t from a normal distribution with unit mean and two units of standard deviation gives glacial cycles with a period of 100 ± 20 kyr, consistent with observations⁴. Terminations are identified from realizations of v_t in the same manner as for the $\delta^{18}\text{O}$ record, except that v_t is first smoothed using an eleven-point running average, and rates of ice volume change must be less than -5 units per kyr. Given these random realizations of termination times, a value of δm is computed from \mathcal{F}_t , and the process repeated 10^5 times to build up a distribution for H_0 (Fig. 1c). This null-distribution of δm is shifted towards positive values because of a tendency for large-amplitude forcing cycles to have a longer period, making H_0 harder to reject than if the nonparametric Wilcoxon rank sum test²² had instead been used.

H_1 is similarly derived from equation (2), but after modifying the threshold condition to be sensitive to insolation forcing, $h_t = 110 - 25\mathcal{F}_t$, and prescribing η_t to have unit variance, which again yields glacial cycles of 100 ± 20 kyr. Under H_1 , terminations tend to trigger when both ice volume and \mathcal{F}_t are large. Termination times calculated according to H_1 are then perturbed using realizations from the stochastic sediment accumulation model consistent with the errors estimated for the depth-derived ages (see Fig. 1a).

The statistical power of the test is measured as the probability of rejecting H_0 at the $P = 0.05$ significance level if H_1 is correct. In the absence of timing errors, the statistical power would be 0.95, but even when timing errors are accounted for, it is still 0.67. Although the power of the test depends upon the form and parameters chosen for the null and alternative models, these results indicate that, unlike for previous tests^{4,11,12}, the combined influence of obliquity and precession will be identifiable, if present. Indeed, the observed value of $\delta m = 0.89$ is highly significant as judged against H_0 ($P = 0.002$) and is near the maximum likelihood value of H_1 (Fig. 1c), even after accounting for errors in timing. Therefore, it is possible to reject the null hypothesis of no orbital influence with a high degree of confidence, and the results are consistent with precession and obliquity together exerting control upon deglaciation.

To explore the sensitivity of these results to different formulations of the orbital forcing, I repeated the test for \mathcal{F}_t computed using all phases of precession and all mixtures of obliquity and precession (Fig. 2). Such combinations reproduce the variability expressed by other measures of insolation forcing, including the caloric summer half-year¹, summer

termination is indicated (red dots), and the median across all such maxima (red dashed line) is 0.89 normalized units greater than the median of the maxima not associated with terminations (black dots and dashed line). **c**, The difference in the medians (vertical grey bar) is highly significant ($P = 0.002$) as judged against the null hypothesis (H_0 , black with the 5% rejection region filled). The difference in medians is also consistent with the alternative hypothesis (H_1 , red lines), whether timing errors are ignored (dashed) or accounted for (solid).

energy¹⁶ (as long as thresholds are not set near peak intensity), and insolation at any particular latitude and on any particular day of the year²³. The resulting contour of significance levels shows highly significant results ($P < 0.01$) in the vicinity of perihelion aligning with the Northern Hemisphere summer solstice and equal contributions from obliquity and precession, though significant results ($P < 0.05$) are also found for perihelion occurring a month earlier or several months later and forcing mixtures having α between 0.3 and 0.9. This shows that any formulation of \mathcal{F}_t in general agreement with Milankovitch's hypothesis would also give a positive result.

To specifically inquire into the ability to reject the null hypothesis of obliquity-only pacing of the glacial cycles, I adopt a null hypothesis wherein the threshold in equation (2) varies according to

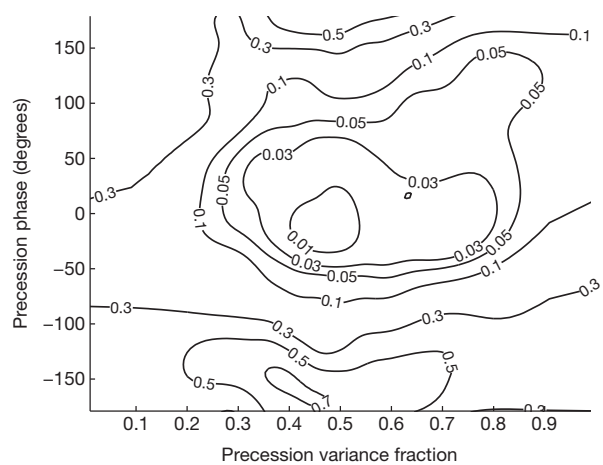


Figure 2 | Sensitivity of the test to choice of orbital forcing. Most orbital forcing curves can be represented as a linear mixture of obliquity and climatic precession (x axis, giving the fraction of precession variance), where climatic precession can take on any phase (y axis, where 0° indicates greatest forcing during the Northern Hemisphere summer solstice). The test's P -value is contoured after applying it to each forcing function. Values less than 0.05 are significant, and the results are consistent with Milankovitch's hypothesis. Forcing functions with a negative obliquity contribution (not shown) are never significant. A two-dimensional smoother was applied to the logarithm of the P -values to make the plot easier to interpret while preserving small values.

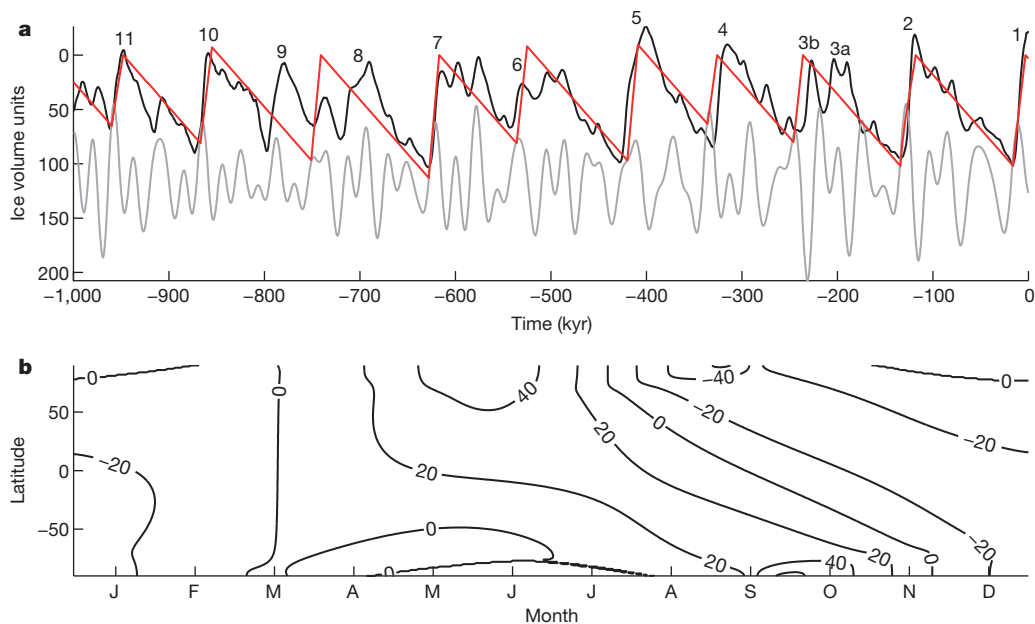


Figure 3 | Orbital forcing of glacial cycles. **a**, A deterministic model of the glacial cycles (red line) using the same threshold condition (grey line) for the alternate hypothesis. For reference, a scaled version of the composite $\delta^{18}\text{O}$ record is also shown (black line). With the exceptions of terminations 3a, 8 and 9 the timing and amplitude of the glacial cycles are generally reproduced. **b**, The

insolation anomaly (in W m^{-2}) that drives deglaciations. Anomalies are computed as the average insolation across the forcing maxima associated with terminations (see Fig. 1) relative to the average insolation over the past million years. Note that anomalies are shown relative to day of the year, not solar longitude³⁰.

$h_t = 105 - 15\epsilon_t$, a formulation consistent with ref. 4 wherein obliquity paces the timing of deglaciation. This formulation shifts the null distribution towards higher values but nonetheless shows $\delta m = 0.89$ to be significant ($P = 0.02$), a result that also holds when any other combination of mean and amplitude is specified for the threshold. Likewise, adoption of a precession-only null hypothesis invariably leads to $\delta m = 0.89$ being significant ($P < 0.01$), regardless of specifications for the mean and amplitude of the threshold and the phase of precession. (The obliquity-only null is harder to reject than the precession-only null because it leads to selection of forcing maxima in \mathcal{F}_t that tend to have the positive phases of both obliquity and precession aligned.) These results show that glacial hypotheses calling singly on precession² or obliquity^{3,4}, or not accounting for either^{13,14}, should be rejected in favour of combined obliquity and precession pacing of late Pleistocene glacial cycles^{1,5–8,10}.

I also repeated the test after updating the depth-derived age model using a compilation of available radiometric constraints upon the age of the last four terminations²⁴. The most significant revision is to shift the ages of terminations 3a and 3b to align with older precession maxima, which increases the mean of the deglacial forcing maxima but has no effect on the median. Therefore, the revised ages do not change the test results, reflecting the test's overall robustness to timing errors. The data and code used to generate each of the above results are available in the Supplementary Information.

The above statistical results can be succinctly illustrated by replacing the stochastic variable in the alternative hypothesis with its mean value and initializing ice volume to be 25 units at $-1,000$ kyr. The resulting deterministic time-history of glaciation gives a cross-correlation of 0.73 with the negative of the $\delta^{18}\text{O}$ record, which is very high relative to other simple model fits given the small number of adjustable parameters²⁵ (Fig. 3a). The model result reproduces the basic sawtooth structure of the late-Pleistocene glacial cycles over the past million years in terms of timing and amplitude, except for terminations 8 and 3b, and illustrates how obliquity, precession and the growth of ice volume can combine to control late-Pleistocene glacial cycles. Another implication is that the climate will tend to be driven out of glaciation sooner when eccentricity—and hence the amplitude of precession—is larger. Because interglacial values of $\delta^{18}\text{O}$ are less

variable than glacial values, this relationship implies that the amplitude of the ~ 100 -kyr glacial cycles are smaller when eccentricity is larger, consistent with the findings reported in ref. 21.

Combined orbital pacing is also consistent with earlier findings that the intervals between successive deglaciations cluster into 80-kyr or 120-kyr periods^{4,11}, indicative of two or three obliquity cycles. Precession, with its ~ 20 -kyr period, achieves a maximum during nearly every interval of above-average obliquity, given the ~ 40 -kyr period of obliquity, but the reverse does not hold. Therefore, precession will tend to influence the precise timing of a deglaciation within an obliquity cycle, but obliquity will more fundamentally govern the interval between deglaciations. Whether precession also influences the precise timing of terminations during the early Pleistocene, when deglaciations occur more nearly every 40 kyr, remains an open question^{16,17}. Perhaps terminations then occurred nearly every time precession maxima coincided with above-average values of obliquity; such a scenario can be obtained by setting the threshold in equation (2) to lower values.

Ice sheets tend to collapse in response to unusually large maxima in insolation forcing that result from the coincidence of high obliquity and alignment of perihelion with Northern Hemisphere summer solstice, consistent with the models hypothesized by Milankovitch¹ and others^{5–10}. During these forcing maxima, summer insolation is as much as 40 W m^{-2} greater at high northern latitudes (Fig. 3b). However, this consistency is not exclusive of all other orbital contributions to deglaciation. For instance, when perihelion aligns with the Northern Hemisphere summer solstice, aphelion occurs during the Southern Hemisphere summer, causing the length of the Southern Hemisphere summer to be longer (Fig. 3b) and, possibly, increasing the escape of CO_2 from the Southern Ocean into the atmosphere^{26–29}. The climate system is thoroughly interconnected across temporal and spatial scales, and, just as neither obliquity nor precession act in isolation, no one region should be expected to exert exclusive influence upon deglaciation.

Received 14 August; accepted 11 October 2011.

1. Milankovitch, M. *Kanon der Erdbestrahlung und seine Anwendung auf das Eiszeitenproblem* 1–503 (Royal Serbian Academy, 1941).
2. Hays, J., Imbrie, J. & Shackleton, N. Variations in the Earth's orbit: pacemaker of the ice ages. *Science* **194**, 1121–1132 (1976).

3. Liu, H. Phase modulation effect of the Rubincam insolation variations. *Theor. Appl. Climatol.* **61**, 217–229 (1998).
4. Huybers, P. & Wunsch, C. Obliquity pacing of the late Pleistocene glacial terminations. *Nature* **434**, 491–494 (2005).
5. Imbrie, J. & Imbrie, J. Modeling the climatic response to orbital variations. *Science* **207**, 943–953 (1980).
6. Paillard, D. The timing of Pleistocene glaciations from a simple multiple-state climate model. *Nature* **391**, 378–381 (1998).
7. Berger, A., Li, X. & Loutre, M. Modelling northern hemisphere ice volume over the last 3Ma. *Quat. Sci. Rev.* **18**, 1–11 (1999).
8. Tziperman, E., Raymo, M., Huybers, P. & Wunsch, C. Consequences of pacing the Pleistocene 100 kyr ice ages by nonlinear phase locking to Milankovitch forcing. *Paleoceanography* **21**, PA4206 (2006).
9. Berger, A. Milankovitch theory and climate. *Rev. Geophys.* **26**, 624–657 (1988).
10. Saltzman, B. *Dynamical Paleoclimatology: Generalized Theory of Global Climate Change* (Academic Press, 2002).
11. Huybers, P. Glacial variability over the last two million years: an extended depth-derived agemodel, continuous obliquity pacing, and the Pleistocene progression. *Quat. Sci. Rev.* **26**, 37–55 (2007).
12. Kawamura, K. *et al.* Northern Hemisphere forcing of climatic cycles in Antarctica over the past 360,000 years. *Nature* **448**, 912–916 (2007).
13. Ghil, M. Cryothermodynamics: the chaotic dynamics of paleoclimate. *Physica D* **77**, 130–159 (1994).
14. Wunsch, C. The spectral description of climate change including the 100ky energy. *Clim. Dyn.* **20**, 353–363 (2003).
15. Herschel, J. On the astronomical causes which may influence geological phenomena. *Trans. Geol. Soc. Lond.* **3**, 293–300 (1832).
16. Huybers, P. Early Pleistocene glacial cycles and the integrated summer insolation forcing. *Science* **313**, 508–511 (2006).
17. Raymo, M., Lisiecki, L. & Nisancioglu, K. Plio-Pleistocene ice volume, Antarctic climate, and the global $\delta^{18}\text{O}$ record. *Science* **313**, (2006).
18. Min, K., Mundil, R., Renne, P. & Ludwig, K. A test for systematic errors in $^{40}\text{Ar}/^{39}\text{Ar}$ geochronology through comparison with U/Pb analysis of a 1.1-Ga rhyolite. *Geochim. Cosmochim. Acta* **64**, 73–98 (2000).
19. Kuiper, K. *et al.* Synchronizing rock clocks of Earth history. *Science* **320**, 500–504 (2008).
20. Broecker, W. In *Milankovitch and Climate* (eds Berger, A. *et al.*) Part 2, 687–698 (D. Riedel, 1984).
21. Lisiecki, L. Links between eccentricity forcing and the 100,000-year glacial cycle. *Nature Geosci.* **3**, 349–352 (2010).
22. Gibbons, J. *Nonparametric Methods for Quantitative Analysis* 1–487 (American Sciences Press, 1985).
23. Imbrie, J. *et al.* On the structure and origin of major glaciation cycles. I: Linear responses to Milankovitch forcing. *Paleoceanography* **7**, 701–738 (1992).
24. Siddall, M., Chappell, J. & Potter, E. In *Developments in Quaternary Science* Vol. 7, 75–92 (Elsevier, 2007).
25. Roe, G. & Allen, M. A comparison of competing explanations for the 100,000-yr ice age cycle. *Geophys. Res. Lett.* **26**, 2259–2262 (1999).
26. Broecker, W. & Henderson, G. The sequence of events surrounding Termination II and their implications for the cause of glacial-interglacial CO_2 changes. *Paleoceanography* **13**, 352–364 (1998).
27. Schulz, K. & Zeebe, R. Pleistocene glacial terminations triggered by synchronous changes in Southern and Northern Hemisphere insolation: the insolation canon hypothesis. *Earth Planet. Sci. Lett.* **249**, 326–336 (2006).
28. Huybers, P. & Denton, G. Antarctic temperature at orbital time scales controlled by local summer duration. *Nature Geosci.* **1**, 787–792 (2008).
29. Timmermann, A., Timm, O., Stott, L. & Meniel, L. The roles of CO_2 and orbital forcing in driving Southern Hemispheric temperature variations during the last 21,000 years. *J. Clim.* **22**, 1626–1640 (2009).
30. Joussaume, S. & Braconnot, P. Sensitivity of paleoclimate simulation results to season definitions. *J. Geophys. Res.* **102**, 1943–1956 (1997).

Supplementary Information is linked to the online version of the paper at www.nature.com/nature.

Acknowledgements This work benefited from comments by G. Gebbie, L. Lisiecki, A. Stine and C. Wunsch.

Author Information Reprints and permissions information is available at www.nature.com/reprints. The author declares no competing financial interests. Readers are welcome to comment on the online version of this article at www.nature.com/nature. Correspondence and requests for materials should be addressed to the author (phuybers@fas.harvard.edu).